Environmental Earth Sciences (2018) 77:398
https://doi.org/10.1007/s12665-018-7579-z

ORIGINAL ARTICLE

Estimating groundwater recharge using GIS-based distributed water balance model in an environmental protection area in the city of Sete Lagoas (MG), Brazil

Paulo Galvão[1] · Ricardo Hirata[2] · Bruno Conicelli[3]

Received: 27 February 2018 / Accepted: 16 May 2018 / Published online: 24 May 2018

Abstract
Improvement in modern water resource management has become increasingly reliant on better characterizing of the spatial variability of groundwater recharge mechanisms. Due to the flexibility and reliability of GIS-based index models, they have become an alternative for mapping and interpreting recharge systems. For this reason, an index model by integrating water balance parameters (surface runoff, actual evapotranspiration, and percolation) calculated by Thornthwaite and Mather's method, with maps of soil texture, land cover, and terrain slope, was developed for a sustainable use of the groundwater resources. The Serra de Santa Helena Environmental Protection Area, next to the urbanized area of Sete Lagoas (MG), Brazil, was selected as the study area. Rapid economic growth has led to the subsequent expansion of the nearby urban area. Large variability in soil type, land use, and slope in this region resulted in spatially complex relationships between recharge areas. Due to these conditions, the study area was divided into four zones, according to the amount of recharge: high (> 100 mm/year), moderate (50–100 mm/year), low (25–50 mm/year), and incipient (> 25 mm/year). The technique proved to be a viable method to estimate the spatial variability of recharge, especially in areas with little to no in situ data. The success of the tool indicates it can be used for a variety of groundwater resource management applications.

Keywords Aquifer recharge · GIS · Water balance model · Environmental protection area · Brazil.

Introduction

The recharge of an aquifer has been defined as the process of addition of water to the saturated zone during a given period. According to Lerner et al. (1990), there are three mechanisms of recharge: direct recharge by percolation through the unsaturated zone, indirect recharge through the beds of surface-water courses, and localized or concentrated recharge at points. Knowledge of an aquifer's recharge is important because it allows for the identification of the water inputs or resources entering the aquifer that can be potentially available for human uses, which are fundamental for appropriate hydrologic planning and water management (Andreo et al. 2008).

Aquifer recharge is a question that is addressed in most manuals of hydrogeology, and in a more specific way, in several books that include detailed information on the estimation of recharge under various climatic and hydrologic circumstances (Freeze and Cherry 1979; Lerner et al. 1990; Fetter 1994; Schwartz and Zhang 2003; Feitosa et al. 2008; Custodio and Llamas 2010; Healy 2010). The process of recharge can be measured by means of diverse methods in which none of these is free from uncertainty (Flint et al. 2002; Scanlon et al. 2002). Direct determinations (e.g., via lysimeters or seepage meters) are of in situ values and not always representative of a whole aquifer. There also exist Darcian approaches based on field measurement and numeric methods using groundwater flow equation under conditions of partial or total saturation (Andreo et al. 2008). Methods based on the use of natural tracers, whether

✉ Paulo Galvão
hidropaulo@gmail.com

[1] Department of Geology, Federal University of Ouro Preto, Morro do Cruzeiro Campus, Ouro Preto, MG 35400-000, Brazil

[2] Groundwater Research Center (CEPAS|USP), Institute of Geosciences, University of São Paulo University of São Paulo, Institute of Geosciences, Rua do Lago 562, São Paulo, SP 05508-080, Brazil

[3] Universidad Regional Amazonica Ikiam, Km 7 Vía Muyuna, Parroquia Muyuna, Tena, Ecuador

chemical (chloride balance) or isotopic (^{18}O, ^{2}H, ^{3}H, and ^{14}C), or whether using artificial tracers (organic and inorganic colorants) constitute an alternative to hydrodynamic methods (Wood and Sanford 1995; Murphy et al. 1996; Scanlon et al. 2002).

Another way of estimating recharge is provided by groundwater balance methods because water entry may be equal to the amount discharged plus (or minus) the variation in the volume of water stored (Blavoux et al. 1992; Samper 1998; Jocson et al. 2002). In practical terms, the balance can be estimated using semi-empirical equations utilizing measurements of precipitation and temperature, indirect estimates of potential and actual evapotranspiration, and effective rainfall (Thornthwaite 1948; Coutagne 1954; Thornthwaite and Mather 1955). Using these approaches, it is possible to estimate the recharge rate of a specific aquifer over extended areas, such as in a scale of a watershed.

Regarding recharge estimations in regional scales, other studies also have used numerical models and flow rate measurements (Sukhila et al. 1996; Birkle et al. 1998; Heathcote et al. 2004; Nolan et al. 2006). In other cases, index methods using GIS-based models to categorize and integrate different parameters (e.g., geological, drainage, soil texture, terrain slope, land cover, and lineaments) have proved to be useful for estimating aquifer recharge spatial distribution (Lin and Anderson 2003; Cherkauer 2004; Batelaan and Smedt 2007; Tilahun and Merkel 2009; Rashid et al. 2012; Rwanga and Ndambuki 2017).

GIS-based index model is a probabilistic representation of nominal values using a Geographic Information System. In other words, it is a simplified representation of a phenomenon or a system based on the use of GIS in the process of building models with spatial data. It is widely used because of the simplification of reality and the extrapolate information to other areas, which can increase the understanding of a system, providing useful guidance and evaluation of scenarios. In this model, values in the form of interval or ratio-scaled variables represent the level of certainty that a feature belongs to a nominal class.

In a hydrologic context, the technique uses GIS to generate the various spatial inputs to the model (e.g., land cover, slope, and soil type), which is commonly used by the United States Geological Survey (Dripps and Bradbury 2007, 2009; Westenbroek et al. 2010). Each parameter used can have different weights according to its features. Depending on the purpose and hydrologic characteristics of the area, the parameters used can be subjective, which many researchers have used different criteria for delineating recharging potential zones.

To illustrate this, Sreedevi et al. (2005) and Srivastava and Bhattacharya (2006) have integrated geophysical data with geospatial data. Nag (2005) has used lineament and hydrogeomorphology-based approach in delineating groundwater potential zones. Jasrotia et al. (2007) and Chenini et al. (2010) have used remote sensing and GIS in delineating artificial recharge sites. Because of the inherent uncertainties of accuracy, a recommendation is that recharge should be estimated using different methods and the results should be compared.

In Brazil, a city named Sete Lagoas (Seven Lakes) faces a rapid economic and population growth, resulting in a subsequent expansion of the urban area which are infringing on protected areas where possibly the local karst aquifer recharge zones are located. Identifying and estimating these zones are important to protect vital resources from contamination and land-use practices that could decrease the quality, quantity, and availability of clean water.

Thus, this paper describes a method for estimating aquifer recharge areas using a GIS-based distributed water balance model conducted in the Serra de Santa Helena Environmental Protection Area (SSHEPA) located in Sete Lagoas, state of Minas Gerais, Brazil. Available information on the database, such as soil texture and land cover were used, as well as slope map by digital altitude model (DAM) was originated. All the data were combined with water balance parameters (runoff, actual evapotranspiration, and percolation) calculated by the Thornthwaite and Mather (1955) method to estimate the aquifer recharge in any area within the SSHEPA to facilitate the strategies for managing groundwater resources.

Site descriptions

The study area is the Serra de Santa Helena Environmental Protection Area (SSHEPA) located in the city of Sete Lagoas, Minas Gerais, Brazil, 70 km northwest of Belo Horizonte, the state capital (Fig. 1). Sete Lagoas has a population estimated greater than 230,000, over an area of 538 km^2 (IBGE 2015), where the greatest population density is in the central, west-central, and north-central areas. The current water supply is almost entirely groundwater from the Sete Lagoas Karst Aquifer (Pessoa 1996; Galvão et al. 2015a) sourced from private and public wells. The public supply wells are managed by the Water Supply and Sewage Service (SAAE) [*SAAE—Serviço Autônomo de Água e Esgoto*].

The SSHEPA is next to the urban area of Sete Lagoas, having an area of about 60 km^2, which represents approximately 10% of the total area of the city (Fig. 1). This protected area is characterized by a very dense and very well-maintained area of transition between the Cerrado biome (constituted by forest savanna, wooded savanna, park savanna, and gramineous-woody savanna) and the Atlantic forest (tropical and subtropical moist broadleaf forests, tropical and subtropical dry broadleaf forests, tropical and subtropical grasslands, and mangrove forests).

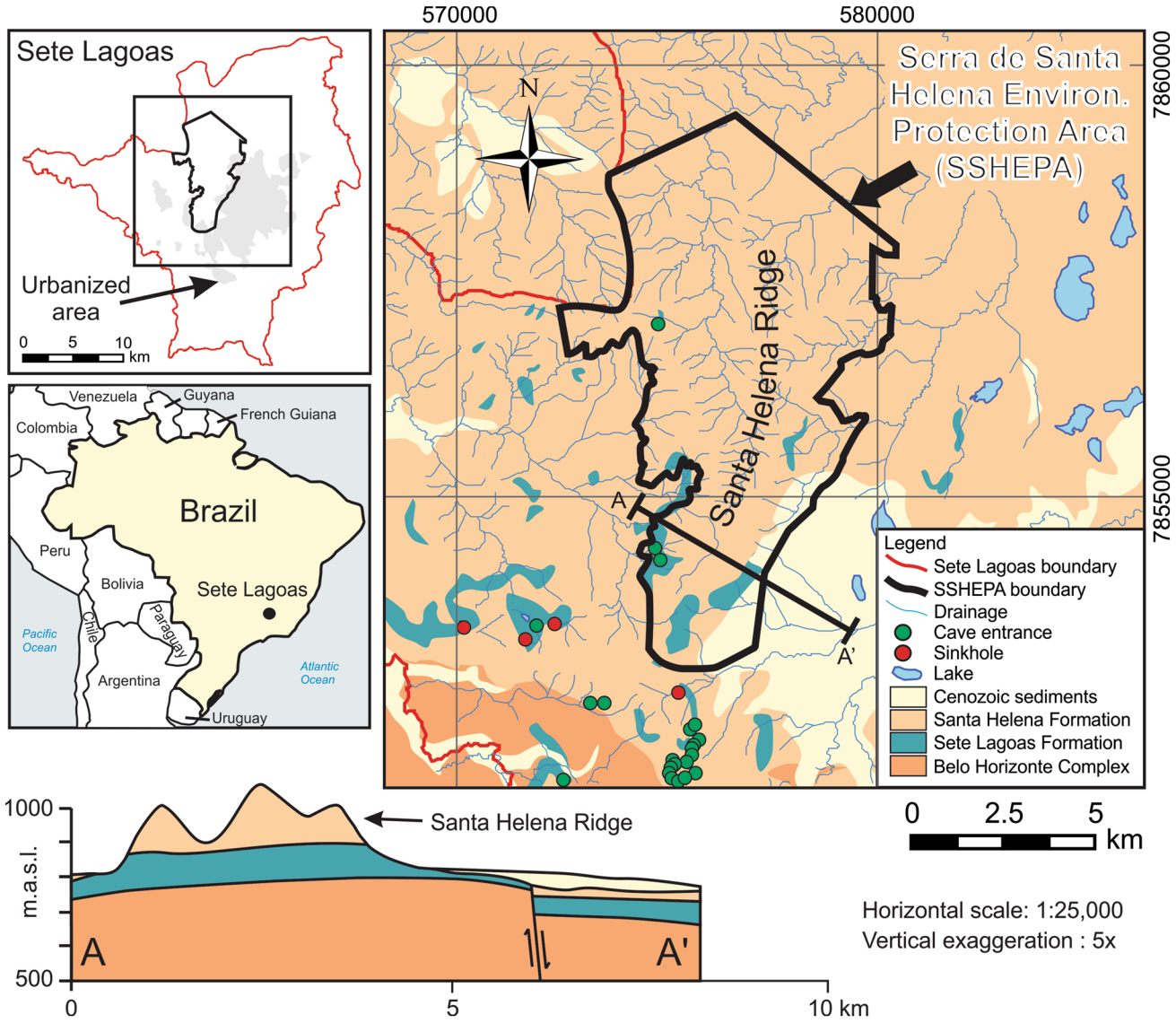

Fig. 1 Location map, in UTM coordinates, of the Serra de Santa Helena Environmental Protection Area (SSHEPA) showing the geology, the drainage pattern, and karst features location (caves entrances and sinkholes). Below the location map, there is a geological cross section (A-A′) showing the lithostratigraphic sequences seen in the study area

Geologically, the SSHEPA is in the São Francisco Craton, where carbonate argillo-arenaceous sediments are emplaced giving origin to the Bambuí Group (Branco and Costa 1961; Oliveira 1967; Schöll and Fogaça 1973; Dardene 1978; Schobbenhaus 1984; Ribeiro et al. 2003; Tuller et al. 2010; Galvão et al. 2016). The Bambuí Group is represented by the lower Sete Lagoas Formation and the upper Serra de Santa Helena Formation. The Sete Lagoas Formation is divided and characterized by two members: Pedro Leopoldo, at the base, composed of fine limestones, dolomites, marlstones, and pelites; and Lagoa Santa, on the top, composed of medium-grained black limestones. The Serra de Santa Helena Formation is constituted of slate, siltstone, and argillite. All the formations are covered by the Cenozoic unconsolidated sediments, which are divided into detritus coverage, alluvial terraces, and alluvium. The area is in a context of basin border, where the basement is represented by gneissic rocks associated with granitoids and migmatite zones from the Belo Horizonte Complex (Tuller et al. 2010) (Fig. 1).

Geomorphologically, the SSHEPA is predominantly characterized by the presence of the Santa Helena Ridge, having denser drainage related to these ridge foothills due to its high slopes. Because the SSHEPA is also in a karst setting area due to the Sete Lagoas Formation, it is common in the presence of lakes, caves, and sinkholes (Pessoa 1996) (Fig. 1).

The Sete Lagoas Karst Aquifer, which is approximately 75 m thick within the urban area of the city, consists of

limestones from the Sete Lagoas Formation. The primary porosity and matrix permeability can be considered very low (Moore 1989), and the secondary porosity is filled by the precipitation of calcite (Tonietto 2010). Most of groundwater flows through karst conducts are characterized as tertiary porosity (Galvão et al. 2015a, b). The Santa Helena Ridge behaves as a watershed boundary, where the eastern portion of the ridge has groundwater flowing to the northeast, while the western portion has groundwater flowing to the northwest (Galvão et al. 2017a).

The mean total monthly precipitation is 106 mm, while the total annual is 1271.8 mm. The rainy season lasts from October to March, with total rainfall of 1132 mm, corresponding to 89% of the annual precipitation. The period with less precipitation lasts from April to September, with 139 mm. The average annual temperature is 20.9 °C, which July has the lowest monthly mean value (17.5 °C) and February the highest one (22.9 °C) (Galvão et al. 2017b). According to Pessoa (1996), the water balance of Sete Lagoas is divided, monthly, in (1) water excess from January to March; (2) water deficit from April to September; and (3) water replacement between October and December, a period of groundwater recharge.

Materials and methods

An index method for distributed recharge integrating water balance in a Geographical Information System was developed, adapting the Fenn et al. (1975) method. In the first stage, a surface runoff map was built overlaying maps of soil, land cover, and terrain slope according to their permeability capacities. For the second stage, a water balance following the Thornthwaite and Mather (1955) method was made to estimate values for different water percolations. In the third and last stage, values of water percolation (calculated in stage 2) to develop the groundwater recharge zone map were established. These methods will be presented below.

Stage 1: estimating spatially runoff classes by index method

Soil permeability map

First, a pedological map of Sete Lagoas (Figs. 2, 3) characterized by six different types of soils (latosol, neosol, cambisol, neosol and cambisol combined, nitosol, and weathered pelitic rock) was analyzed, and then based on its characteristics and percentage of clay/silt or organic matter were reclassified. Soils with high clay/silt content were considered impermeable, with low or zero infiltration capacity, while soils with low clay/silt-sized particles were considered as permeable, or with high infiltration capacity. After reclassification, a second map of soil permeability was developed considering only two classes: (1) sandy (high permeability or low runoff) and (2) silty (low permeability or high runoff).

Land cover infiltration capacity map

A land cover map of Sete Lagoas was analyzed, and then classified land cover classes found within the SSHEPA based on its phytophysionomy formations (Ribeiro and Walter 2008), such as grassy, forest, savanna, and anthropic. These formations consequently were reclassified according to their capacity for infiltration, resulting in a second map composed of two classes: (1) forest and savannah (high permeability or low runoff) and (2) anthropic and grassy formations (low permeability or high runoff) (Figs. 2, 4).

Terrain slope map by Digital Altitude Model

Digital Altitude Model (DAM) map was made. A local map of topographic elevations using a SRTM image (Shuttle Radar Topography Mission), Sheet SE-23-Z-C, acquired from EMBRAPA's website (http://www.relevobr.cnpm.embrapa.br) was extracted using Global Mapper 11 software, and then the DAM was originated using ArcGIS 10.5 software. Three slope intervals were defined, according to the American Society of Civil Engineers (1969): $<2\%$—low slopes; 2–7%—moderate slopes, and $>7\%$—high slopes (Figs. 2, 5).

The final surface runoff map

The shapefiles corresponding to the maps of soil permeability, land cover infiltration capacity, and terrain slope were entered in a GIS database, georeferenced in the ArcGIS 10.5 software. After that, they were converted into raster formats, and then integrated using the raster calculator tool of the ArcGIS considering their respective classes, generating a final surface runoff map composed of 12 classes (Figs. 2, 6). The coordinate system used was Universal Transverse Mercator (UTM) projection, Zone 23, datum SAD 69, with units in meters.

Stage 2: water balance estimations for each class of the surface runoff map

The water balance method proposed by Thornthwaite and Mather (1955) is one of the most widely used, especially due to its low input requirements and coherent estimates of water balance components. The procedure allows estimating the actual evapotranspiration, soil water deficit and excess, and percolation. For the paper, water balances were estimated for each type of class of the final surface runoff map,

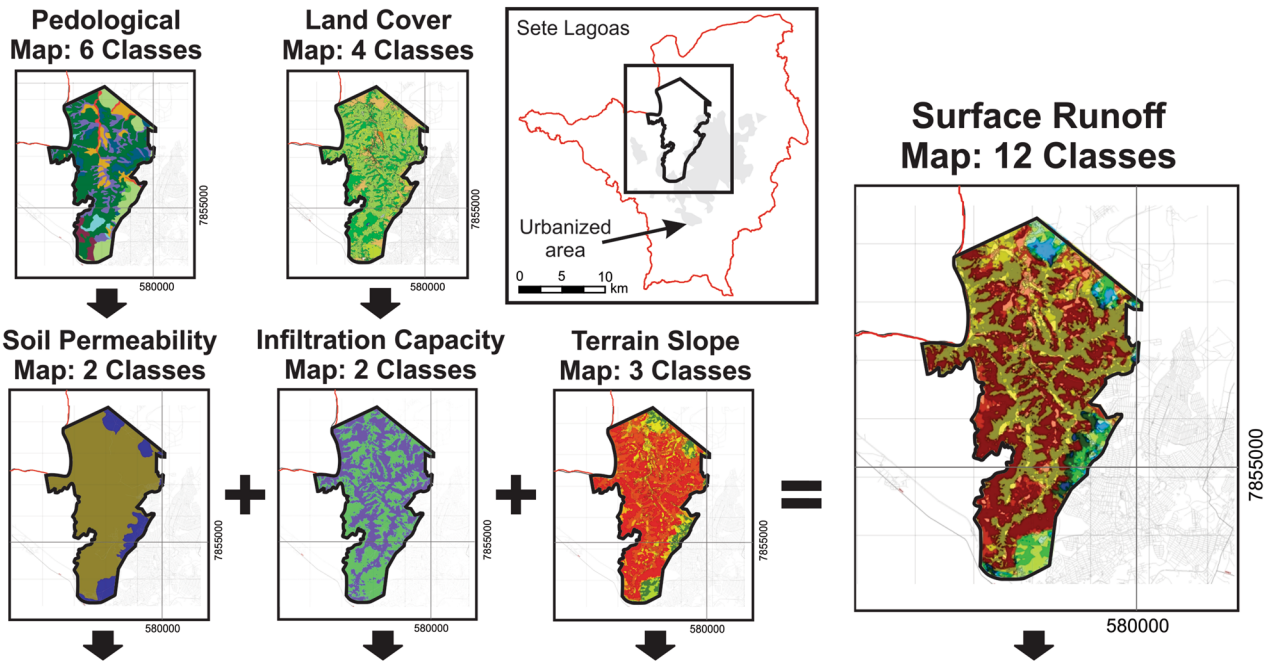

Soil Permeability	Land Cover Infiltration Capacity	Terrain Slope (%)	Classification
Sandy	Forest Formation Savannah Formation	< 2	Class 1
		2 - 7	Class 2
		> 7	Class 3
	Anthropic Formation Grassy Formation	< 2	Class 4
		2 - 7	Class 5
		> 7	Class 6
Silty	Forest Formation Savannah Formation	< 2	Class 7
		2 - 7	Class 8
		> 7	Class 9
	Anthropic Formation Grassy Formation	< 2	Class 10
		2 - 7	Class 11
		> 7	Class 12

Fig. 2 Schematic representation of the surface runoff map by overlaying maps of soil permeability, land cover infiltration, and terrain slope. Pedological map was reclassified according to infiltration capacities, resulting in the soil permeability map. Land cover infiltration capacity map, based on the land cover map, was classified into similar infiltration capacities. Terrain slope map was a result of a digital altitude model where intervals were defined according to the American Society of Civil Engineers (1969)

according to the following water balance equation $P = Q + E + \Delta S$, where: P is the precipitation (mm); Q is the streamflow, or surface runoff (mm); E is the evapotranspiration (mm); and ΔS is the changes in storage in the soil, or in the bedrock (mm).

According to Fenn et al. (1975), the Thornthwaite and Mather (1955) method "*centers around the amount of free water present in the soil. Until the field capacity of a soil is reached, the moisture in the soil is regarded as being a balance between what enters it as a result of precipitation and what leaves through evapotranspiration. If the monthly moisture loss from the soil through evapotranspiration is compared with the monthly precipitation, an accounting of the soil moisture can be made by a simple bookkeeping procedure*" (such as the use of predefined tables of soil moisture retention values).

For the water balance estimations using the Thornthwaite and Mather (1955) method and adapted for the study area's approach, some components of the calculation sheet (see rows on Tables 4, 5, 6, 7, 8, 9) should be mentioned and commented:

Row A: average monthly precipitation (PRE) Historical series of the INMET—EMBRAPA Climate Station (Climate Normals data from 1961 to 1990—Table 1), located

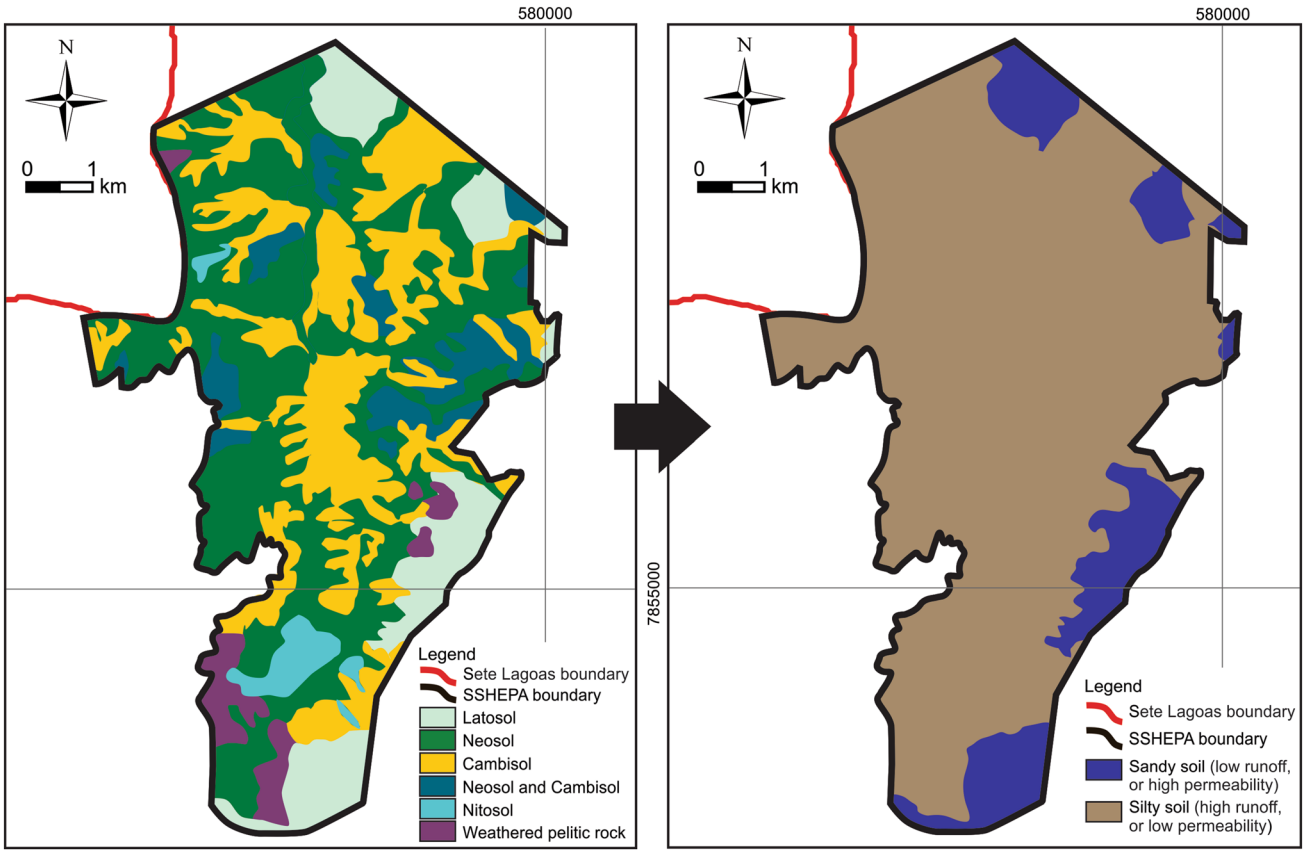

Fig. 3 Pedological map of Sete Lagoas (left) and its distributions of soil permeabilities (right)

in the city of Sete Lagoas (coordinates UTM: 23K 586760E, 7847260S, elevation 735 m).

Row B: average monthly temperature (T) Average monthly temperature (°C) also based on the INMET—EMBRAPA's Climate Normals (Table 1).

Row C: potential evapotranspiration (PET) The maximum amount of water capable of being lost as steam by a continuous medium of vegetation that covers the entire surface of the soil that reached the field capacity of a soil. This amount is determined through derivations of the Thornthwaite (1948) method and associated with its defined data tables (for more details, see pages 126–130, 138, from Koerner and Daniel 1997).

Row D: runoff coefficient (C) The amount of precipitation that flows on the surface before being infiltrated into the soil. In practice, *C* can be obtained from an empirical determination of rational method. Many similar tabulations of runoff coefficient may be found in the literature. One of the most used is that proposed by the American Society of Civil Engineers (1969) (Table 2). The selection of an appropriated coefficient is based on the study area features. From Table 2, *C* values for each type of class found in the final surface runoff map were discriminated, according to the equation $C = 1 - (C'_1 + C'_2 + C'_3)$ (column 5, Table 3) for water balance calculations (column 6, Table 3). Due to the study area features, only two values of *C* (sand and silt—Table 2) were adopted in the second column of Table 3 (C'_1 = soil permeability). In the third column of Table 3 (C'_2 = land cover infiltration capacity), the item "forest/savannah formation" can be related to the "forest riparian/reforestation" item from the Table 2, due to its similar permeability capacity (low runoff), while "anthropic/grassy Formation" (Table 3) can be related to the "cultivated fields; lawn" (moderate/high runoff) (Table 2). The fourth column (C'_3 = terrain slope—Table 3) adopted values of Slope from Table 2.

Row E: surface runoff (SR) The part of the runoff that travels over the soil surface to the nearest stream channel, being part of the runoff of a drainage basin that has not passed beneath the surface since precipitation. It is calculated by multiplying the respective values of *PRE* (*Row A*) and *C* (*Row D*).

Row F: infiltration (IN) The amount of precipitation that enters through the surface of the soil cover. It is assumed to equal *PRE* minus *SR* (*Row A* − Row *E*).

Row G: infiltration minus potential evapotranspiration (IN − PET) To determine periods of excess and deficit of soil moisture, it is necessary to obtain the difference between infiltration (*Row F*) and potential evapotranspiration (*Row*

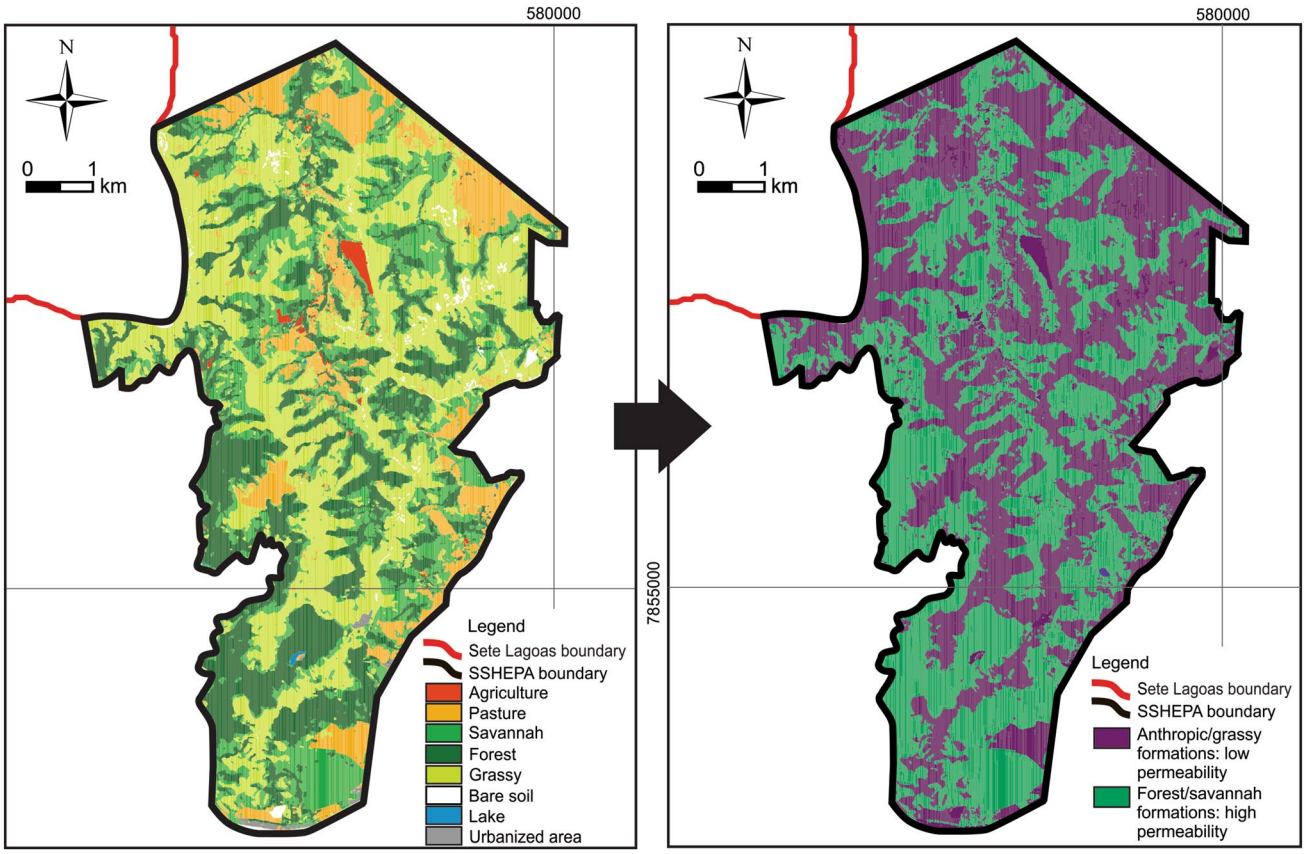

Fig. 4 Distribution of land covers (left) and its distributions of infiltration capacity (right)

C). Positive numbers indicate potential accumulation (storage) of water in the cover soil (i.e., more infiltration than potential evapotranspiration). If $IN - PET$ is negative, then the soil is drying.

Row H: accumulated water loss (WL) It is the sum of the negative monthly values of $IN - PET$ starting in January (*Row G*). If the value is greater than or equal to zero, enter 0.0 in *WL Row*, and then go to the next month. If the value of $IN - PET$ is negative, enter the negative value.

Row I: field capacity of soil (FC) The amount of soil moisture or water content held in the soil a few days after having been wetted and after free drainage has ceased, without producing continuous downward percolation. For the study area, the *FC* value adopted was 150 mm, due to the soil features and the predominance of vegetation with shallow roots (for more details on how to compute the values on the FC Row, see pages 131–136 from Koerner and Daniel 1997).

Row J: FC change Represents the change in soil moisture, month by month. In other words, the *FC* in a month minus the *FC* in the previous month (*Row I*).

Row K: water deficit (WD) When evapotranspiration is in excess of precipitation and any previously available moisture has been used, in soil moisture utilization. It is the difference between $IN - PET$ (*Row G*) and *FC change* (*Row J*), when $IN - PET$ is negative.

Row L: actual evapotranspiration (AET) The quantity amount of water actually removed from a surface due to processes of evaporation and transpiration of a given month. It is the difference between *PET* (*Row C*) and *WD* (*Row K*).

Row M: percolation (P) After FC reaches its maximum, any excess infiltration becomes into percolation through the soil cover until reaching deeper regions. Significant percolations will occur during the months when the infiltration exceeds the precipitation ($IN - PET$ is positive) and the soil moisture exceeds its maximum. It is the difference between *PET* (*Row G*) and *WD* (*Row J*), when $IN - PET$ is positive.

Stage 3: groundwater recharge map of SSHEPA

For the estimation of zones with different recharge rates in the SSHEPA, the parameters surface runoff (SR), actual evapotranspiration (AET), and percolation (P) were used for each class established in the surface runoff map (Stage 1, Fig. 6) and applied to the equations of water balance (Stage 2), resulting in 12 potential percolation values (Tables 3, 4, 5, 6, 7, 8, 9). Based on these, it was possible to gather these 12 classes in 4

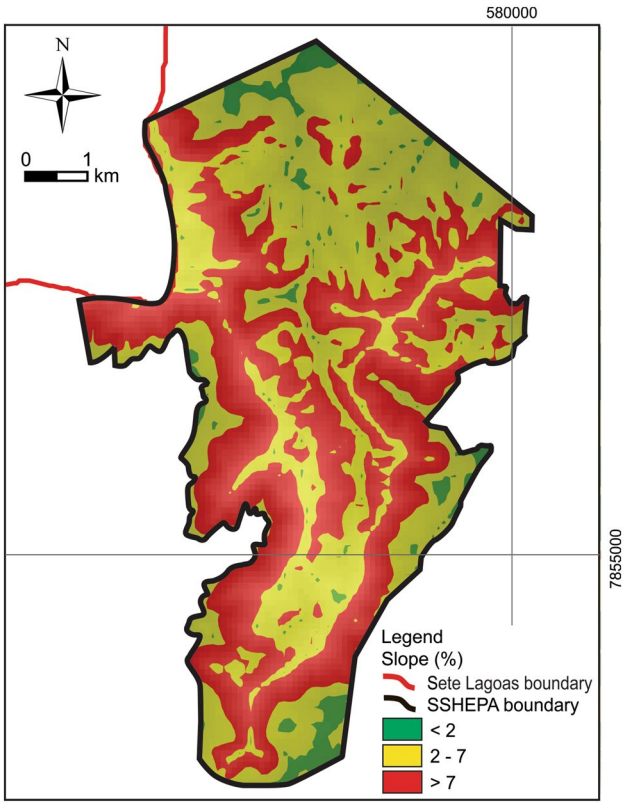

Fig. 5 Terrain slope map by digital altitude model indicating predominance for slopes between 2 and 7%, or above 7%

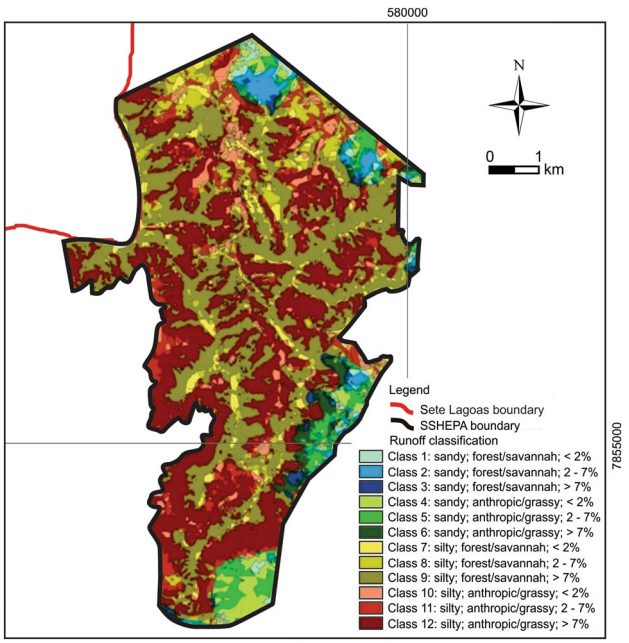

Fig. 6 Final surface runoff map, a result of integration of maps of soil permeability, land cover infiltration capacity, and terrain slope

Table 1 Three-decade (1961–1990) monthly averages of climatologic variables including precipitation, *PRE* (mm) and temperature, *T* (°C) for Sete Lagoas Climate Station

INMET—EMBRAPA climate station—Sete Lagoas		
Month	Mean *PRE* (mm)	Mean *T* (°C)
Jan	251.80	22.70
Feb	172.60	22.90
Mar	106.30	22.70
Apr	49.30	21.10
May	23.90	19.00
Jun	7.80	17.80
Jul	16.40	17.50
Aug	11.80	19.40
Sep	30.10	21.00
Oct	120.90	22.10
Nov	224.20	22.30
Dec	256.70	22.40
Total average	105.98	20.91
Accumulated	1271.80	–

Table 2 Values for runoff coefficient (*C*) from the American Society of Civil Engineers (1970) tabulation that is adaptable for the study area

Type of area	C'
Soil (C'_1)	
Clay	0.1
Silt	0.2
Sand	0.4
Land cover (C'_2)	
Cultivated fields/lawn	0.1
Forest riparian/reforestation	0.2
Slope (%) (C'_3)	
< 2	0.3
2–7	0.2
> 7	0.1

zones of interest in the final groundwater recharge map of the SSHEPA (Fig. 7):

- Zone 1—high recharge rates: > 100 mm/year;
- Zone 2—moderate recharge rates: 50–100 mm/year;
- Zone 3—low recharge rates: 25–50 mm/year;
- Zone 4—incipient recharge rates: > 25 mm/year.

Table 3 Values of C calculated for the study area based on Table 2. The lower is the surface runoff coefficient, the higher is the permeability capacity

Classification	C'_1 = soil permeability	C'_2 = land cover infiltration capacity	C'_3 = terrain slope (%)	$C = 1 - (C'_1 + C'_2 + C'_3)$	C = runoff coefficient
Class 1	Sandy	Forest/savannah formation	< 2	1 − (0.4 + 0.2 + 0.3)	0.1
Class 2			2–7	1 − (0.4 + 0.2 + 0.2)	0.2
Class 3			> 7	1 − (0.4 + 0.2 + 0.1)	0.3
Class 4		Anthropic/grassy formation	< 2	1 − (0.4 + 0.1 + 0.3)	0.2
Class 5			2–7	1 − (0.4 + 0.1 + 0.2)	0.3
Class 6			> 7	1 − (0.4 + 0.1 + 0.1)	0.4
Class 7	Silty	Forest/savannah formation	< 2	1 − (0.2 + 0.2 + 0.3)	0.3
Class 8			2–7	1 − (0.2 + 0.2 + 0.2)	0.4
Class 9			> 7	1 − (0.2 + 0.2 + 0.1)	0.5
Class 10		Anthropic/grassy formation	< 2	1 − (0.2 + 0.1 + 0.3)	0.4
Class 11			2–7	1 − (0.2 + 0.1 + 0.2)	0.5
Class 12			> 7	1 − (0.2 + 0.1 + 0.1)	0.6

Results and discussion

Stage 1: estimating spatially runoff classes by index method

Soil permeability map

Soil texture reflects the particle size distribution of a soil. In general, the higher the percentage of silt- and clay-sized particles, the higher the water holding capacity, which is controlled primarily by the soil texture and the soil organic matter content (Leeper and Uren 1993; Charman and Murphy 2000), resulting in low values of permeability. The small particles (clay and silt) have a much larger surface area than the larger sand particles. This large area allows the soil to hold a greater quantity of water, but the capacity to infiltrate water is very low, increasing the surface runoff.

The soil permeability map (Fig. 3, right), based on pedological map of Sete Lagoas (Fig. 3, left) reveals that areas constituted majority by sandy soils (latosol) are in the peripheries of the area, while the rest of the SSHELA is covered by soils predominantly silty (neosol, cambisol, nitosol, and weathered pelitic rocks).

Land cover infiltration capacity map

Land covers have a great impact on infiltration and runoff. Vegetation can slow the movement of runoff, allowing more time for it to seep into the ground (Allen 1997). Impervious surfaces, such as parking lots, roads, and urban areas act as a "fast lane" for rainfall draining the water directly into streams (Fetter 1994). Agriculture and the tillage of land also change the infiltration patterns of a landscape. Water that, in natural conditions, infiltrated directly into the soil now runs off into streams.

The land cover map (Fig. 4, left) indicates that most of the ridge area is covered by grassy vegetation, while pasture areas are in the peripheries of the area, coinciding mostly to regions with sandy soils (Fig. 3). Reclassifying the map according to their capacity for infiltration, resulting in the infiltration capacity map (Fig. 4, right), the distributions of potential high permeabilities match with forest and savannah areas, where ridge foothills are commons, while low permeabilities match with anthropic and grassy formations in more planar areas.

Terrain slope map by digital altitude model (DAM)

Every watershed is surrounded by a topography divide (ridge line), which fixes the area of catchment from which the surface runoff takes place. The slope of the topography of the watershed is one of the most important factors that control the time of overland flow and concentration of runoff in the main stream. If the slope is high, the velocity of overland flow will also be high interfering in the infiltration, which will be low (Das and Saikia 2013). In the case of low slope values, the velocity of overland flow is also low resulting in more time for infiltration and even the presence of accumulating depressions slowing runoff.

The DAM map reveals that, at least, half part of the SSHEPA is in moderate slopes, between 2 and 7%, followed by high slopes, > 7%, due to the steepest parts of the ridge, while planar areas, < 2%, are the minority (Fig. 5).

Table 4 Water balance calculation for Class 1 adopting runoff coefficient equal to 0.1

Class 1 (Runoff coefficient, $C = 0.1$)															
Row	Parameter	Reference	Jan	Feb	Mar	Apr	May	Jun	Jul	Aug	Sep	Oct	Nov	Dec	Average	Total
A	Avg. monthly pre.—PRE (mm)	Input data*	251.8	172.6	106.3	49.3	23.9	7.8	16.4	11.8	30.1	120.9	224.2	256.7	106.0	**1271.8**
B	Avg. Monthly Temp.—T (°C)	Input data*	22.7	22.9	22.7	21.1	19.0	17.8	17.5	19.4	21.0	22.1	22.3	22.4	20.9	–
C	Potential evapotranspiration—PET (mm)	Thornthwaite (1948) Method	112.9	99.0	104.0	78.6	60.5	52.4	48.5	65.3	81.0	97.2	101.4	106.0	83.9	1006.7
D	Runoff coefficient—C	See Tables 2 and 3 (this case, C = 0.1)	0.1	0.1	0.1	0.1	0.1	0.1	0.1	0.1	0.1	0.1	0.1	0.1	–	–
E	Surface runoff—SR (mm)	SR = Row A × Row D	25.2	17.3	10.6	4.9	2.4	0.8	1.6	1.2	3.0	12.1	22.4	25.7	10.6	**127.2**
F	Infiltration—IN (mm)	IN = Row A − Row E	226.6	155.3	95.7	44.4	21.5	7.0	14.8	10.6	27.1	108.8	201.8	231.0	95.4	1144.6
G	IN − PET (mm)	= Row F − Row C	113.8	56.3	− 8.3	− 34.2	− 39.0	− 45.4	− 33.7	− 54.7	− 53.9	11.6	100.4	125.0	–	–
H	Accumulated water loss—WL (mm)	WL = ΣNeg (I − PET)	0.0	0.0	− 8.3	− 42.5	− 81.5	− 126.9	− 160.6	− 215.3	− 269.2	0.0	0.0	0.0	–	–
I	Field capacity of soil—FC (mm)	FC = 150 mm (adopted for the area)	150.0	150.0	141.7	111.9	85.5	62.4	49.5	33.9	23.4	35.0	135.4	150.0	–	–
J	FC change (mm)	FC actual − FC previous month	0.0	0.0	− 8.3	− 29.8	− 26.4	− 23.0	− 13.0	− 15.6	− 10.5	11.6	100.4	14.6	–	–
K	Water deficit—WD (mm)	WD = Row G − Row J, when Row G is negative	0.0	0.0	− 0.1	4.4	12.6	22.4	20.7	39.1	43.4	0.0	0.0	0.0	11.9	142.6
L	Actual Evapotranspiration—AET (mm)	AET = Row C − Row K	112.9	99.0	104.0	74.2	47.9	30.0	27.7	26.2	37.6	97.2	101.4	106.0	72.0	**864.1**
M	Percolation—P (mm)	P = Row G − Row J, when Row G is positive	113.8	56.3	0.0	0.0	0.0	0.0	0.0	0.0	0.0	0.0	0.0	110.4	23.4	**280.5**

Parameter in bold to separate results to apply in the equation PRE = SR + ETR + P (1271.8 = 127.2 + 864.1 + 280.5)

– not applicable

*Climate normals data from 1961 to 1990, INMET—EMBRAPA Climate Station, located in Sete Lagoas (coordinates UTM: 23K 586760E, 7847260S, elevation 735 m)

Table 5 Water balance calculation for Classes 2 and 4 adopting runoff coefficient equal to 0.2

Classes 2, 4 (runoff coefficient, $C = 0.2$)															
Row	Parameter	Reference	Jan	Feb	Mar	Apr	May	Jun	Jul	Aug	Sep	Oct	Nov	Dec	Average	Total
A	Avg. monthly Pre.—PRE (mm)	Input data*	251.8	172.6	106.3	49.3	23.9	7.8	16.4	11.8	30.1	120.9	224.2	256.7	106.0	**1271.8**
B	Avg. monthly temp.—T (°C)	Input data*	22.7	22.9	22.7	21.1	19.0	17.8	17.5	19.4	21.0	22.1	22.3	22.4	20.9	-
C	Potential evapotranspiration—PET (mm)	Thornthwaite (1948) Method	112.9	99.0	104.0	78.6	60.5	52.4	48.5	65.3	81.0	97.2	101.4	106.0	83.9	1006.7
D	Runoff coefficient—C	See Tables 2 and 3 (this case, $C = 0.1$)	0.2	0.2	0.2	0.2	0.2	0.2	0.2	0.2	0.2	0.2	0.2	0.2	-	-
E	Surface runoff—SR (mm)	SR = Row A × Row D	50.4	34.5	21.3	9.9	4.8	1.6	3.3	2.4	6.0	24.2	44.8	51.3	21.2	**254.4**
F	Infiltration—IN (mm)	IN = Row A − Row E	201.4	138.1	85.0	39.4	19.1	6.2	13.1	9.4	24.1	96.7	179.4	205.4	84.8	1017.4
G	IN − PET (mm)	= Row F − Row C	88.6	39.1	− 18.9	− 39.1	− 41.4	− 46.2	− 35.3	− 55.9	− 56.9	− 0.5	78.0	99.3	–	–
H	Accumulated water loss—WL (mm)	WL = ΣNeg (I − PET)	0.0	0.0	− 18.9	− 58.0	− 99.4	− 145.6	− 180.9	− 236.8	− 293.8	− 294.2	0.0	0.0	–	–
I	Field capacity of soil—FC (mm)	FC = 150 mm (adopted for the area)	150.0	150.0	131.6	100.5	75.5	54.9	43.0	29.2	19.7	19.7	97.6	150.0	–	–
J	FC change (mm)	FC actual − FC previous month	0.0	0.0	− 18.4	− 31.2	− 25.0	− 20.6	− 11.9	− 13.8	− 9.5	− 0.1	78.0	52.4	–	–
K	Water deficit—WD (mm)	WD = Row G − Row J, when Row G is negative	0.0	0.0	0.0	8.0	16.4	25.6	23.4	42.1	47.4	0.5	0.0	0.0	13.6	163.5
L	Actual evapotranspiration—AET (mm)	AET = Row C − Row K	112.9	99.0	104.0	70.6	44.1	26.9	25.0	23.2	33.6	96.7	101.4	106.0	70.3	**843.2**
M	Percolation—P (mm)	P = Row G − Row J, when Row G is positive	88.6	39.1	0.0	0.0	0.0	0.0	0.0	0.0	0.0	0.0	0.0	47.0	14.6	**174.6**

Parameter in bold to separate results to apply in the equation PRE = SR + ETR + P (1271.8 = 254.4 + 843.2 + 174.6)

– not applicable

*Climate normals data from 1961 to 1990, INMET—EMBRAPA Climate Station, located in Sete Lagoas (coordinates UTM: 23K 586760E, 7847260S, elevation 735 m)

Table 6 Water balance calculation for Classes 3, 5 and 7 adopting runoff coefficient equal to 0.3

Classes 3, 5, 7 (runoff coefficient, $C = 0.3$)															
Row	Avg. monthly pre.—PRE (mm)	Input data*	Jan	Feb	Mar	Apr	May	Jun	Jul	Aug	Sep	Oct	Nov	Dec	Average	Total
A	Avg. Monthly Temp.—T (°C)	Input data*	251.8	172.6	106.3	49.3	23.9	7.8	16.4	11.8	30.1	120.9	224.2	256.7	106.0	**1271.8**
B	Potential evapotranspiration—PET (mm)	Thornthwaite (1948) Method	22.7	22.9	22.7	21.1	19.0	17.8	17.5	19.4	21.0	22.1	22.3	22.4	20.9	–
C	Runoff coefficient—C	See Tables 2 and 3 (this case, C = 0.1)	112.9	99.0	104.0	78.6	60.5	52.4	48.5	65.3	81.0	97.2	101.4	106.0	83.9	1006.7
D	Surface runoff—SR (mm)	SR = Row A × Row D	0.3	0.3	0.3	0.3	0.3	0.3	0.3	0.3	0.3	0.3	0.3	0.3	–	–
E	Infiltration—IN (mm)	IN = Row A − Row E	75.5	51.8	31.9	14.8	7.2	2.3	4.9	3.5	9.0	36.3	67.3	77.0	31.8	**381.5**
F	IN − PET (mm)	= Row F − Row C	176.3	120.8	74.4	34.5	16.7	5.5	11.5	8.3	21.1	84.6	156.9	179.7	74.2	890.3
G	Accumulated water loss—WL (mm)	WL = ΣNeg (I − PET)	63.4	21.8	− 29.5	− 44.1	− 43.8	− 47.0	− 37.0	− 57.1	− 59.9	− 12.6	55.6	73.7	–	–
H	Field capacity of soil—FC (mm)	FC = 150 mm (adopted for the area)	0.0	0.0	− 29.5	− 73.6	− 117.4	− 164.3	− 201.3	− 258.4	− 318.3	− 330.9	0.0	0.0	–	–
I	FC change (mm)	FC actual − FC previous month	150.0	150.0	122.3	90.2	66.7	48.2	37.3	25.2	16.6	15.3	70.8	144.5	–	–
J	Water deficit—WD (mm)	WD = Row G − Row J, when Row G is negative	− 5.5	0.0	− 27.7	− 32.1	− 23.5	− 18.5	− 10.9	− 12.2	− 8.5	− 1.4	55.6	73.7	–	–
K	Actual Evapotranspiration—AET (mm)	AET = Row C − Row K	0.0	0.0	1.9	12.0	20.2	28.5	26.1	44.9	51.4	11.2	0.0	0.0	16.3	196.1
L	Percolation—P (mm)	P = Row G − Row J, when Row G is positive	112.9	99.0	102.1	66.6	40.3	23.9	22.3	20.4	29.6	86.0	101.4	106.0	67.5	**810.5**
M	Avg. monthly pre.—PRE (mm)	Input data*	57.9	21.8	0.0	0.0	0.0	0.0	0.0	0.0	0.0	0.0	0.0	0.0	6.6	**79.7**

Parameter in bold to separate results to apply in the equation PRE = SR + ETR + P (1271.8 = 381.5 + 810.5 + 79.7)

– not applicable

*Climate normals data from 1961 to 1990, INMET—EMBRAPA Climate Station, located in Sete Lagoas (coordinates UTM: 23K 586760E, 7847260S, elevation 735 m)

Table 7 Water balance calculation for Classes 6, 8 and 10 adopting runoff coefficient equal to 0.4

Classes 6, 8, 10 (runoff coefficient, $C = 0.4$)															
Row	Avg. monthly pre.—PRE (mm)	Input data*	Jan	Feb	Mar	Apr	May	Jun	Jul	Aug	Sep	Oct	Nov	Dec	Average	Total
A	Avg. Monthly Temp.—T (°C)	Input data*	251.8	172.6	106.3	49.3	23.9	7.8	16.4	11.8	30.1	120.9	224.2	256.7	106.0	**1271.8**
B	Potential evapotranspiration—PET (mm)	Thornthwaite (1948) Method	22.7	22.9	22.7	21.1	19.0	17.8	17.5	19.4	21.0	22.1	22.3	22.4	20.9	–
C	Runoff coefficient—C	See Tables 2 and 3 (this case, C = 0.1)	112.9	99.0	104.0	78.6	60.5	52.4	48.5	65.3	81.0	97.2	101.4	106.0	83.9	1006.7
D	Surface runoff—SR (mm)	SR = Row A × Row D	0.4	0.4	0.4	0.4	0.4	0.4	0.4	0.4	0.4	0.4	0.4	0.4	–	–
E	Infiltration—IN (mm)	IN = Row A − Row E	100.7	69.0	42.5	19.7	9.6	3.1	6.6	4.7	12.0	48.4	89.7	102.7	42.4	**508.7**
F	IN − PET (mm)	= Row F − Row C	151.1	103.6	63.8	29.6	14.3	4.7	9.8	7.1	18.1	72.5	134.5	154.0	63.6	763.1
G	Accumulated water loss—WL (mm)	WL = ΣNeg (I − PET)	38.2	4.6	− 40.2	− 49.0	− 46.1	− 47.8	− 38.6	− 58.3	− 62.9	− 24.7	33.2	48.0	–	–
H	Field capacity of soil—FC (mm)	FC = 150 mm (adopted for the area)	0.0	0.0	− 40.2	− 89.2	− 135.3	− 183.1	− 221.7	− 279.9	− 342.9	− 367.5	0.0	0.0	–	–
I	FC change (mm)	FC actual − FC previous month	150.0	150.0	113.7	81.0	58.9	42.4	32.4	21.7	14.0	11.8	45.0	93.0	–	–
J	Water deficit—WD (mm)	WD = Row G − Row J, when Row G is negative	0.0	0.0	− 36.3	− 32.6	− 22.1	− 16.6	− 9.9	− 10.7	− 7.6	− 2.2	33.2	48.0	–	–
K	Actual Evapotranspiration—AET (mm)	AET = Row C − Row K	0.0	0.0	3.8	16.4	24.0	31.2	28.7	47.5	55.3	22.5	0.0	0.0	19.1	229.4
L	Percolation—P (mm)	P = Row G − Row J, when Row G is positive	112.9	99.0	100.1	62.2	36.5	21.2	19.8	17.8	25.7	74.7	101.4	106.0	64.8	**777.3**
M	Avg. monthly pre.—PRE (mm)	Input data*	38.2	4.6	0.0	0.0	0.0	0.0	0.0	0.0	0.0	0.0	0.0	0.0	3.6	**42.8**

Parameter in bold to separate results to apply in the equation PRE = SR + ETR + P (1271.8 = 508.7 + 720.3 + 42.8)

– not applicable

*Climate normals data from 1961 to 1990, INMET—EMBRAPA Climate Station, located in Sete Lagoas (coordinates UTM: 23K 586760E, 7847260S, elevation 735 m)

Table 8 Water balance calculation for Classes 9 and 11 adopting runoff coefficient equal to 0.5

Classes 9, 11 (runoff coefficient, $C = 0.5$)															
Row	Parameter	Reference	Jan	Feb	Mar	Apr	May	Jun	Jul	Aug	Sep	Oct	Nov	Dec	Average	Total
A	Avg. monthly pre.—PRE (mm)	Input data*	251.8	172.6	106.3	49.3	23.9	7.8	16.4	11.8	30.1	120.9	224.2	256.7	106.0	**1271.8**
B	Avg. Monthly Temp.—T (°C)	Input data*	22.7	22.9	22.7	21.1	19.0	17.8	17.5	19.4	21.0	22.1	22.3	22.4	20.9	–
C	Potential evapotranspiration—PET (mm)	Thornthwaite (1948) Method	112.9	99.0	104.0	78.6	60.5	52.4	48.5	65.3	81.0	97.2	101.4	106.0	83.9	1006.7
D	Runoff coefficient—C	See Tables 2 and 3 (this case, C = 0.1)	0.5	0.5	0.5	0.5	0.5	0.5	0.5	0.5	0.5	0.5	0.5	0.5	–	–
E	Surface runoff—SR (mm)	SR = Row A × Row D	125.9	86.3	53.2	24.7	12.0	3.9	8.2	5.9	15.1	60.5	112.1	128.4	53.0	**635.9**
F	Infiltration—IN (mm)	IN = Row A − Row E	125.9	86.3	53.2	24.7	12.0	3.9	8.2	5.9	15.1	60.5	112.1	128.4	53.0	635.9
G	IN − PET (mm)	= Row F − Row C	13.0	− 12.7	− 50.8	− 53.9	− 48.5	− 48.5	− 40.3	− 59.4	− 66.0	− 36.8	10.7	22.3	–	–
H	Accumulated water loss—WL (mm)	WL = ΣNeg (I − PET)	0.0	− 12.7	− 63.5	− 117.4	− 166.0	− 214.5	− 254.7	− 314.2	− 380.1	− 416.9	0.0	0.0	–	–
I	Field capacity of soil—FC (mm)	FC = 150 mm (adopted for the area)	150.0	137.4	96.7	66.7	47.7	34.1	25.8	17.1	10.9	8.4	19.2	41.5	–	–
J	FC change (mm)	FC actual − FC previous month	0.0	− 12.6	− 40.7	− 30.1	− 19.0	− 13.6	− 8.3	− 8.7	− 6.3	− 2.4	10.7	22.3	–	–
K	Water deficit—WD (mm)	WD = Row G − Row J, when Row G is negative	0.0	0.1	10.1	23.8	29.5	35.0	32.0	50.7	59.7	34.3	0.0	0.0	22.9	275.3
L	Actual Evapotranspiration—AET (mm)	AET = Row C − Row K	112.9	98.9	93.8	54.7	30.9	17.5	16.5	14.6	21.3	62.9	101.4	106.0	60.9	**731.4**
M	Percolation—P (mm)	P = Row G − Row J, when Row G is positive	13.0	0.0	0.0	0.0	0.0	0.0	0.0	0.0	0.0	0.0	0.0	0.0	1.1	**13.0**

Parameter in bold to separate results to apply in the equation PRE = SR + ETR + P (1271.8 = 635.9 + 731.4 + 13.0)

– not applicable

*Climate normals data from 1961 to 1990, INMET—EMBRAPA Climate Station, located in Sete Lagoas (coordinates UTM: 23K 586760E, 7847260S, elevation 735 m)

Table 9 Water balance calculation for Class 12 adopting Runoff Coefficient equal to 0.6

Class 12 (runoff coefficient, $C = 0.6$)															
Row	Parameter	Reference	Jan	Feb	Mar	Apr	May	Jun	Jul	Aug	Sep	Oct	Nov	Dec	Average	Total
A	Avg. monthly pre.—PRE (mm)	Input data*	251.8	172.6	106.3	49.3	23.9	7.8	16.4	11.8	30.1	120.9	224.2	256.7	106.0	**1271.8**
B	Avg. Monthly Temp.—T (°C)	Input data*	22.7	22.9	22.7	21.1	19.0	17.8	17.5	19.4	21.0	22.1	22.3	22.4	20.9	–
C	Potential evapotranspiration—PET (mm)	Thornthwaite (1948) Method	112.9	99.0	104.0	78.6	60.5	52.4	48.5	65.3	81.0	97.2	101.4	106.0	83.9	1006.7
D	Runoff coefficient—C	See Tables 2 and 3 (this case, C = 0.1)	0.6	0.6	0.6	0.6	0.6	0.6	0.6	0.6	0.6	0.6	0.6	0.6	–	–
E	Surface runoff—SR (mm)	SR = Row A × Row D	151.1	103.6	63.8	29.6	14.3	4.7	9.8	7.1	18.1	72.5	134.5	154.0	63.6	**763.1**
F	Infiltration—IN (mm)	IN = Row A − Row E	100.7	69.0	42.5	19.7	9.6	3.1	6.6	4.7	12.0	48.4	89.7	102.7	42.4	508.7
G	IN − PET (mm)	= Row F − Row C	− 12.1	− 30.0	− 61.4	− 58.9	− 50.9	− 49.3	− 41.9	− 60.6	− 69.0	− 48.8	− 11.7	− 3.3	–	–
H	Accumulated water loss—WL (mm)	WL = ΣNeg (I − PET)	− 12.1	− 42.1	− 103.5	− 162.4	− 213.3	− 262.6	− 304.5	− 365.1	− 434.1	− 482.9	− 494.6	− 498.0	–	–
I	Field capacity of soil—FC (mm)	FC = 150 mm (adopted for the area)	137.9	95.8	0.0	0.0	0.0	0.0	0.0	0.0	0.0	0.0	0.0	0.0	–	–
J	FC change (mm)	FC actual − FC previous month	137.9	− 42.1	− 95.8	0.0	0.0	0.0	0.0	0.0	0.0	0.0	0.0	0.0	–	–
K	Water deficit—WD (mm)	WD = Row G − Row J, when Row G is negative	150.1	− 12.1	− 34.4	58.9	50.9	49.3	41.9	60.6	69.0	48.8	11.7	3.3	41.5	498.0
L	Actual Evapotranspiration—AET (mm)	AET = Row C − Row K	− 37.2	111.1	138.4	19.7	9.6	3.1	6.6	4.7	12.0	48.4	89.7	102.7	42.4	**508.7**
M	Percolation—P (mm)	P = Row G − Row J, when Row G is positive	0.0	0.0	0.0	0.0	0.0	0.0	0.0	0.0	0.0	0.0	0.0	0.0	0.0	**0.0**

Parameter in bold to separate results to apply in the equation PRE = SR + ETR + P (1271.8 = 763.1 + 508.7 + 0.0)

– not applicable

*Climate normals data from 1961 to 1990, INMET - EMBRAPA Climate Station, located in Sete Lagoas (coordinates UTM: 23K 586760E, 7847260S, elevation 735 m)

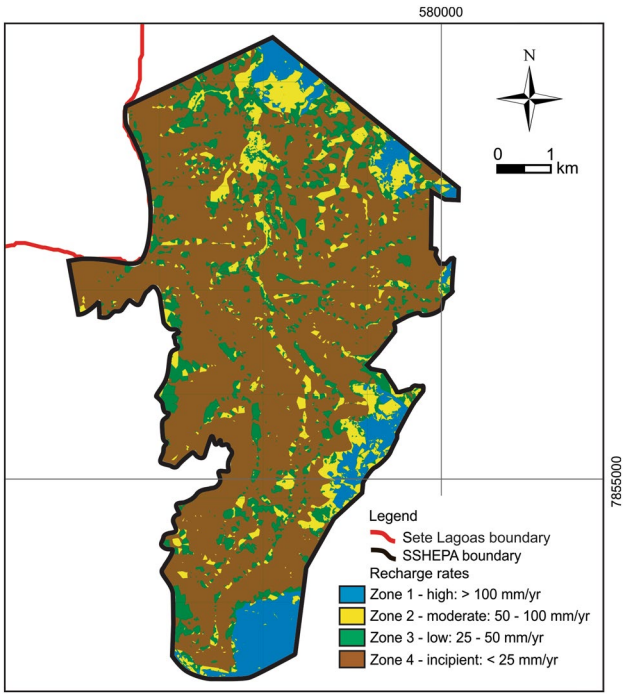

Fig. 7 Final groundwater recharge map of the SSHEPA. Note zone 1, with high recharge rates, is in the northern, eastern and southern portions of the APASSH, near the urban area of Sete Lagoas, while zone 4 covers most part of the area where the highest rectilinear slopes of the ridge are located

The final surface runoff map

From integration of maps of soil permeability, land cover infiltration capacity, and terrain slope, a final surface runoff map (Fig. 6) revels 12 different classes with different runoff coefficients, *C*, that may be coincident according to the combinations of features of soils, land covers, and terrain slope (Table 3).

Stage 2: water balance estimations for each class of the surface runoff map

As the final surface runoff map (Fig. 6) revels 12 different classes which coincide in 6 values of runoff coefficient, ($C = 0.1$–0.6), to estimate the total annual amount of percolation, and hence the recharge rates, six water balances were calculated according to their respective runoff coefficients (Tables 4, 5, 6, 7, 8, 9).

The results indicated the lower is the runoff coefficient (such as in the classes 1, 2, and 4), the lower are the surface runoffs and actual evapotranspiration rates, and the higher is the percolation values. Classes with high runoff coefficients (9, 11, 12) tend to present low percolation annual rates, and consequently high values of surface runoff and actual evapotranspiration (Table 10).

Stage 3: groundwater recharge map of SSHEPA

Zone 1 (blue, Fig. 7) includes classes 1, 2, and 4, and indicates high recharge rates, with values above 100 mm/year. It occurs mainly in areas where the features of soil, land cover, and terrain slope are suitable for a significant percolation of surface water, such as in sandy soils, slopes < 2% and 2–7%, and forest cover. The fact that one class included in this zone shows significant percolation and yet in an anthropic/grassy formation area (Class 4, Table 3), it is compensated by the low slope and the sandy character of the terrain. This zone

Table 10 Annual values for precipitation, surface runoff, actual evapotranspiration, and percolation for each of the 12 classes

Classification	Runoff coefficient	Parameter (mm/year)			
		Precipitation	Surface runoff	actual evapotranspiration	Percolation
Class 1	0.1	1271.8	127.2	864.1	280.5
Class 2	0.2	1271.8	254.4	843.2	174.6
Class 3	0.3	1271.8	381.5	810.5	79.7
Class 4	0.2	1271.8	254.4	843.2	174.6
Class 5	0.3	1271.8	381.5	810.5	79.7
Class 6	0.4	1271.8	508.7	777.3	42.8
Class 7	0.3	1271.8	381.5	810.5	79.7
Class 8	0.4	1271.8	508.7	777.3	42.8
Class 9	0.5	1271.8	635.9	731.4	13.0
Class 10	0.4	1271.8	508.7	777.3	42.8
Class 11	0.5	1271.8	635.9	731.4	13.0
Class 12	0.6	1271.8	763.1	508.7	0.0

Note that the higher is the runoff coefficient, the greater is the surface runoff and actual evapotranspiration, and the lower is the percolation value. The same colors indicate coincidences in results

can be found in the northern, eastern, and southern portions of APASSH, near the urban area of Sete Lagoas.

Zone 2 (yellow, Fig. 7) includes classes 3, 5, and 7, and indicates moderate recharge rates, with values between 50 and 100 mm/year. It occurs in sandy and silty areas, with terrain slopes between 2 and 7%, and in both forest/savannah and anthropic/grassy areas. In areas with silty soils (Class 7, Table 3), which reduces the capacity of percolation, it is compensated by the presence of forest/savannah areas and low slopes, while in areas with moderate slopes and without much presence of forests are compensated by the sandy soil. This zone can be seen surrounding Zone 1, near hills with predominantly convex slope forms, in the higher and lower regions of the SSHEPA.

Zone 3 (green, Fig. 7) includes classes 4, 6, and 8, and indicates low recharge rates, with values from 25 to 50 mm/year, due to areas with moderate and high slopes, silty soils (and consequently less permeable than sandy soils), and in anthropic/grassy formation area. In forest/savannah regions (Class 6, Table 3), which could increase the percolation, the potential for water absorption is reduced by moderate terrain slopes soil type. This zone can be identified as several small zones dispersed on the SSHEPA and in the steepest parts of the hills.

Zone 4 (brown, Fig. 7) includes classes 9, 11, and 12, and indicates incipient recharge rates, with values below 25 mm/year. This is because it presents a combination of silty soils, high terrain slopes, and predominant anthropic/grassy areas, which considerably reduce the field capacity of the soil, and therefore a significant percolation rate. This zone covers most of the area where the highest slopes of the ridge characterized by rectilinear forms are located.

Although some areas have low recharge rates and consequently high surface runoff, they are close to zones of high and moderate recharge rates, which means that waters drained over these low recharge zones at higher altitudes can reach areas with lower elevations and high percolation capacities. This, coupled with the geologic features and its stratigraphic position (slate, siltstone and argillite of the Serra de Santa Helena Formation covering limestones of the Sete Lagoas Formation, Fig. 1) turn the SSHEPA, as a whole, an important recharge area for the Sete Lagoas Aquifer (in this case, an allogenic recharge type), where this aquifer is the main source of water supply for the city.

It is important to mention that, due to the inexistence of information about streamflow hydrographs within the area, a field validation for the index model developed in this paper was not possible to make. The final objective of the paper is not to present a definitive recharge map of the SSHEPA, but, based on the GIS-based index model, a simplified representation of the reality to help to predict impacts of alternative management actions, such as land-use planning, site selections, and to identify areas of possible concerns.

It is known by preview studies that in the central urbanized area of Sete Lagoas the groundwater extraction during several decades of pumping resulted in a considerable cone of depression and locally vadose karst conduct zones, which explains the emergence of the cluster of induced subsidence or collapse events (Galvão et al. 2015b). A significant part of this exploited groundwater is recharging from the SSHEPA, confirmed by stable isotopes and hydrogeochemical data (Galvão et al. 2017b).

Based on these issues, some recommendations for the sustainable use of the groundwater resources are suggested. In the case of Zone 1 (high recharge rates), and the nearest of the urbanized area, recommendations include reducing or avoiding new occupations, and hence drilling new wells, prioritizing existing public wells to supply, and switching to surface water supply where possible. The main concern is to not decrease the quality and quantity of groundwater downstream, as recharge areas also are pathways for contaminants, mainly in karst areas that are highly susceptible. The moderate recharge Zone 2, especially in forest/savannah and low slopes areas, should also be preserved in terms of quality and quantity of groundwater because these areas are located upstream and surrounding Zone 1. Any type of contamination or high pumping rate wells should consequently impact the Zone 1. The Zones 3 and 4, which are occupying the majority of the SSHEPA, due to a combination of silty soils and high terrain slopes, they are naturally less vulnerable for contamination and inappropriate areas for living, respectively. Because of this, the areas should be monitored for possible disorderly occupations and geotechnical events.

Conclusions

The study has established the interrelationships between groundwater recharge factors and the GIS-based distributed water balance model, which produced a groundwater recharge potential map of the Serra de Santa Helena Environmental Protection Area. This method proved to be a viable tool, especially in areas with little to no in situ data.

The results indicated that the most effective groundwater recharge potential zone is located downstream (near the urban area of Sete Lagoas), where areas with features of soil, land cover, and terrain slope are suitable for a significant percolation of surface water, such as sandy soils, slopes < 2% and 2–7%, and forest cover. Upstream regions are least effective for groundwater recharge, mainly due to silty soils, high terrain slopes, and predominant anthropic/grassy areas. This combination considerably reduces field capacities of the soil, and therefore a significant percolation rate.

Some limitations of the method should be mentioned: (1) the scale adopted can be considered large (about 60 km^2). Thus, owing to the resolution of certain maps, the final map

may present possible discrepancies in certain boundaries of the recharge zones; (2) since groundwater recharge is directly correlated with percolation, the established values should be more accurate if the rate of percolation or hydraulic conductivity of each recharge zone can be confirmed on-site; (3) as the area is in a context of karst region, some features (e.g., cave entries and sinkholes) should be considered as zones with high recharge rates. However, due to the scale, these features were not considered; and (4) the final map should be compared with other GIS methods with different criteria.

Acknowledgements This work was supported by Biopreservação Consultoria e Empreendimentos. Special thanks go to Gustavo Ganzaroli Mahé, Sidney Schaberle Goveia, and Kyle Spears.

References

Allen PA (1997) Earth surface processes. Blackwell Sciences, Oxford, 404 p

Andreo B, Vías JM, Durán JJ, Jiménez P, López-Geta JA, Carrasco F (2008) Methodology for groundwater recharge assessment in carbonate aquifers: application to pilot sites in southern Spain. Hydrogeol J 16:911–925

ASCE—American Society of Civil Engineers (1969) Task force on effect of urban development on flood discharges, committee on flood control, "effect of urban development on flood discharges—current knowledge and future needs", J Hydraul Division, 95 (HY1), 287–309

Batelaan O, De Smedt F (2007) GIS-based recharge estimation by coupling surface-subsurface water balances. J Hydrol 337:337–355

Birkle P, Torres Rodríguez V, González Partida E (1998) The water balance for the basin of the valley of Mexico and implications for future water consumption. Hydrogeol J 6(4):500–517

Blavoux B, Mudry J, Puig JM (1992) Budget, functioning and protection of Fontaine de Vaucluse system (south-east France) (in French). Geodin Acta 5(3):153–172

Branco Jr, Costa MT (1961) Belo Horizonte-Brasilia road map tour. Brazilian Congress of Geology, Brasilia. Radioactive Research Institute, Federal University of Minas Gerais (UFMG), Publication 15, Belo Horizonte, p 25

Charman PEV, Murphy BW (2000) Soils: their properties and management, 2nd edn. Oxford University Press, Melbourne, 448p

Chenini I, Benmammou A, Elmay M (2010) Groundwater recharge zone mapping using GIS-based multi-criteria analysis: a case study in central Tunisia (Maknassy Basin). Int J Water Resour Manag 24:921–939

Cherkauer DS (2004) Quantifying ground water recharge at multiple scales using PRMS and GIS, Ground Water, vol 42, 1, pp 97–110

Coutagne A (1954) Study of some regional hydrometereological correlations and their algebraic interpretation (in French)

Custodio E, Llamas MR (2001) Hidrologia subterrânea. Tomo I e II, Ediciones Omega. S.A, Barcelona. 2350p

Dardene MA (1978) Synthesis on the stratigraphy of Bambuí Group in Central Brazil. Brazilian Congress of Geology, 30, Recife. Annals Recife: Brazilian Society of Geology, 1978 v.2, pp 597–610

Das MM, Saikia MD (2013) Watershed management. PHI Learning Private Limited. 303p

Dripps W, Bradbury K (2007) A simple, daily soil–water balance model for estimating the spatial and temporal distribution of ground water recharge in temperate humid areas. Hydrogeol J 15(3):433–444

Dripps W, Bradbury K (2009) The spatial and temporal variability of ground water recharge in a forested basin in Northern Wisconsin. Hydrol Process 24(4):383–392

Feitosa FAC (2008) Hidrogeologia: conceitos e aplicações [Hydrogeology: concepts and aplications, 3rd edn. CPRM, Rio de Janeiro, 812p LABHID.

Fenn DG, Hanley KJ, De Geare TV (1975) Use of the Water Balance Method for predicting leachate generation from solid waste disposal sites. US Environmental Protection Agency, Report No. EPA/530/SW168

Fetter CW (1994) Applied hydrogeology, 616. Macmillan College Publishing, Inc., New York

Flint AL, Flint LE, Kwicklis EM, Fabryka-Martin JT, Bodvarsson GS (2002) Estimating recharge at Yucca Mountain, Nevada, USA: comparison of methods. Hydrogeol J 10(1):180–204

Freeze AR, Cherry JA (1979) Groundwater: Englewood Cliffs, New Jersey, Prentice-Hall, 604

Galvão P, Halihan T, Hirata R (2015a) The Karst Permeability Scale Effect of Sete Lagoas, MG, Brazil. J Hydrol 531:85/15–105. https://doi.org/10.1016/j.jhydrol.2015.11.026

Galvão P, Halihan T, Hirata R (2015b) Evaluating karst geotechnical risk in the urbanized area of Sete Lagoas, Minas Gerais, Brazil. Hydrogeol J 23(7):1499–1513

Galvão P, Hirata R, Cordeiro A, Osório DB, Peñaranda J (2016) Geologic conceptual model of the municipality of Sete Lagoas (MG, Brazil) and the surroundings. Anais da Academia Brasileira de Ciências 88(1):35–53

Galvão P, Halihan T, Hirata R (2017a) Transmissivity of aquifer by capture zone method: an application in the Sete Lagoas Karst Aquifer, MG, Brazil. Anais da Academia Brasileira de Ciências, v. 89, pp 91–102

Galvão P, Hirata R, Halihan T, Terada R (2017b) Recharge sources and hydrochemical evolution of an urban karst aquifer, Sete Lagoas, MG, Brazil. Environ Earth Sci 76:159. https://doi.org/10.1007/s12665-017-6482-3

Healy RW (2010) Estimating groundwater recharge. Cambridge University Press, Cambridge, 264

Heathcote JA, Lewis RT, Soley RWN (2004) Rainfall routing to runoff and recharge for regional groundwater resource models. Q J Eng Geol Hydrogeol 37(2):113–130

Jasrotia AS, Kumar R, Saraf AK (2007) Delineation of groundwater recharge sites using integrated remote sensing and GIS in Jammu district, India. Int J Remote Sens 28(22):5019–5036

Jocson JMU, Jenson JW, Contractor DN (2002) Recharge and aquifer response: northern Guam Lens Aquifer, Guam Mariana Islands. J Hydrol 260:231–254

Koerner RM, Daniel DE (1997) Final covers for solid waste landfills and abandoned dumps. ASCE Press, Reston, 256 p

Leeper GW, Uren NC (1993) Soil science: an introduction, 5th edn. Melbourne University Press, Melbourne, 312p

Lerner DN, Issar AS, Simmers I (1990) Groundwater recharge: a guide to understanding and estimating natural recharge. International Contributions to Hydrogeology 8. Heise, Hannover

Lin Y-F, Anderson MP (2003) A digital procedure for ground water recharge and discharge pattern recognition and rate estimation. ground water, vol 41, 3, pp 306–315

Murphy EM, Ginn TR, Phillips JL (1996) Geochemical estimates of palaeo recharge in the Pasco Basin: evolution of the chloride mass balance technique. Water Resour Res 32(9):2853–2868

Nag SK (2005) Application of lineament density and hydrogeomorphology to delineate groundwater potential zones of Baghmundi block in Purulia district, West Bengal. J Indian Soc Rem Sens 33(4):522–529

Nolan BT, Healy RV, Taber PE, Perkins K, Hitt KJ, Wolock DM (2006) Factors influencing ground-water recharge in the eastern United States. J Hydrol 332(1–2):187–205. https://doi.org/10.1016/j.hydrol.2006.06.029

Oliveira MAM (1967) Contribution to the geology of the southern part of the São Francisco Basin and adjacent areas. Collection of Reports Exploration, Rio de Janeiro 1: Petrobras, n.3, pp 71–105

Pessoa P (1996) Hydrogeological characterization of the region of Sete Lagoas - MG: Potentials and Risks. Master Thesis. Department of Geosciences, University of São Paulo. São Paulo

Rashid M, Lone MA, Ahmed S (2012) Integrating geospatial and ground geophysical informationas guidelines for groundwater potential zones in hard rock terrains of south India. Environ Monit Assess 184:4829–4839. https://doi.org/10.1007/s10661-011-2305-2

Ribeiro JF, Walter BMT (2008) As principais fitofisionomias do Bioma Cerrado. In: Almeida SP, Ribeiro JF (eds) Cerrado: ecologia e flora [The main vegetation types of the Cerrado. In Cerrado: ecologyand flora]. SM Sano, Embrapa-CPAC, Planaltina, pp 151–212

Ribeiro JH, Tuller MP, Danderfer Filho A (2003) Geological mapping of the region of Sete Lagoas, Pedro Leopoldo, Matozinhos, Lagoa Santa, Vespasiano, Capim Branco, Prudente de Morais, Confins and Funilândia, Minas Gerais State, Brazil (scale1:50,000). 2nd edn. Belo Horizonte. 54 p

Rwanga SS, Ndambuki JM (2017) Approach to quantify groundwater recharge using gis based water balance model: a review. Int J Adv Agric Environ Eng (IJAAEE) 4:Issue 1

Samper J (1998) Evaluation of recharge from rainfall using water balances: utilization, calibration and uncertainties (in Spanish). Bol Geol Miner 109:347–370

Scanlon BR, Healy RW, Cook PG (2002) Choosing appropriate techniques for quantifying groundwater recharge. Hydrogeol J 10:18–39

Schobbenhaus C (1984) Geology of Brazil. National Department of Mineral Production, pp 275–277

Schöll WU, Fogaça ACC (1973) Stratigraphy of the Espinhaço in the Diamantina region. In: Symposium on Geology of Minas Gerais State, Brazil, 1. Acts. Belo Horizonte: Brazilian Geology Society p 55–73 [Bulletin. 1]

Schwartz FW, Zhang H (2003) Fundamentals of ground water. Wiley, New York

Sharma ML (1990) Groundwater recharge. Balkema, Rotterdam

Srivastava PK, Bhattacharya AK (2006) Groundwater assessment through an integrated approach using remote sensing, using remote sensing, GIS and resistivity techniques: a case study from a hard rock terrain. Int J Remote Sens 27(20):4599–4620

Sukhija BS, Nagabhushanam P, Reddy DV (1996) Groundwater recharge in semi-arid regions of India: an overview of results obtained using tracers. Hydrogeol J 4(3):50–71

Thornthwaite CW (1948) An approach towards a rational classification of climate. Geogr Rev 38:55–94

Thornthwaite CW, Mather JR (1955) The water balance. Publications in climatology. Laboratory of climatology. New Gersey 8:104

Tilahun K, Merkel BJ (2009) Estimation of groundwater recharge using a GIS-based distributed water balance model in Dire Dawa, Ethiopia Hydrogeol J 17:1443–1457. https://doi.org/10.1007/s10040-009-0455-x

Tucci CEM, Barros MT, Porto RL (1995) Drenagem Urbana. Ed., Porto Alegre, Universidade/UFRGS, 414 p

Tuller MP, Ribeiro JH, Signorelli N, Féboli WL, Pinho JMM (2010) Sete Lagoas—Abaeté Project, Minas Gerais State, Brazil. 6 geological maps, scale 1:100.000 (Geology Program of Brazil), 160p

Westenbroek SM, Kelson VA, Dripps WR, Hunt RJ, Bradbury KR, 2010. SWB—a modified thornthwaite-Mather Soil-Water-Balance Code for Estimating Groundwater Recharge: U.S. Geological Survey Techniques and Methods 6-A31, 60 p

Wood WW, Sanford WE (1995) Chemical and isotopic methods for quantifying groundwater recharge in a regional, semiarid environment. Ground Water 33:458–468

IBGE—Brazilian Institute of Geography and Statistics (2015) Basic Municipal Information.Available: http://www.cidades.ibge.gov.br/xtras/perfil.php?lang=&codmun=316720&search=minas-gerais|sete-lagoas. Accessed Oct 2016